

# A Reanalysis of Public Galactic Bulge Gravitational Microlensing Events from OGLE-III and -IV

Golovich, Dawson, Bartolic et al. (2022, ApJS, 260, 2)

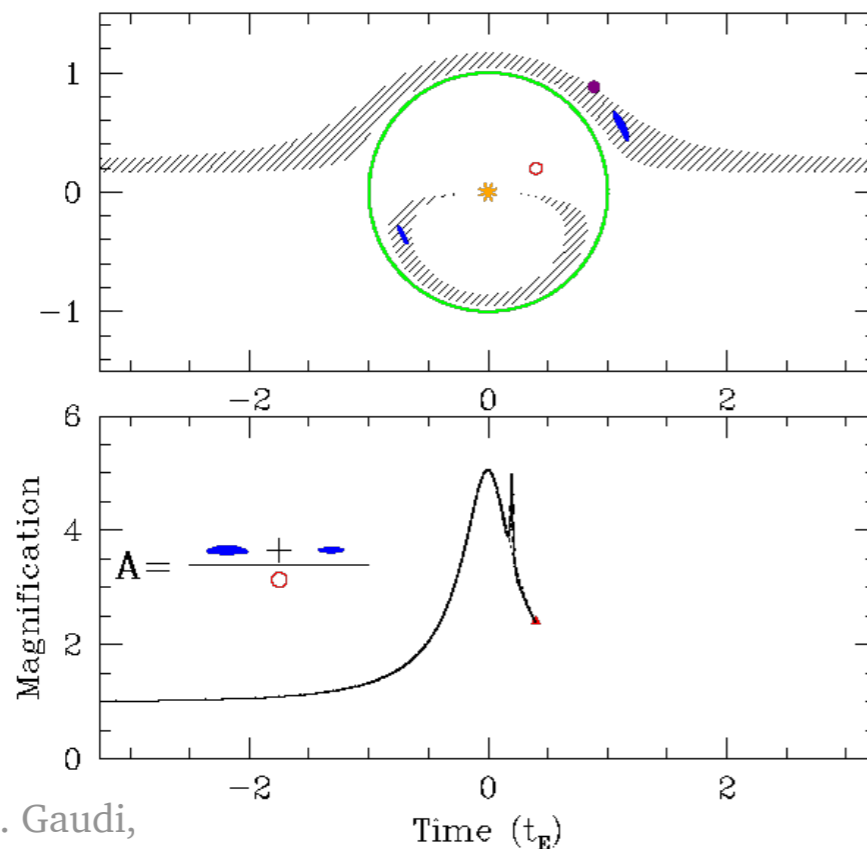
# Problematics in studies of $t_E$ distribution

## (Abstract + Introduction)

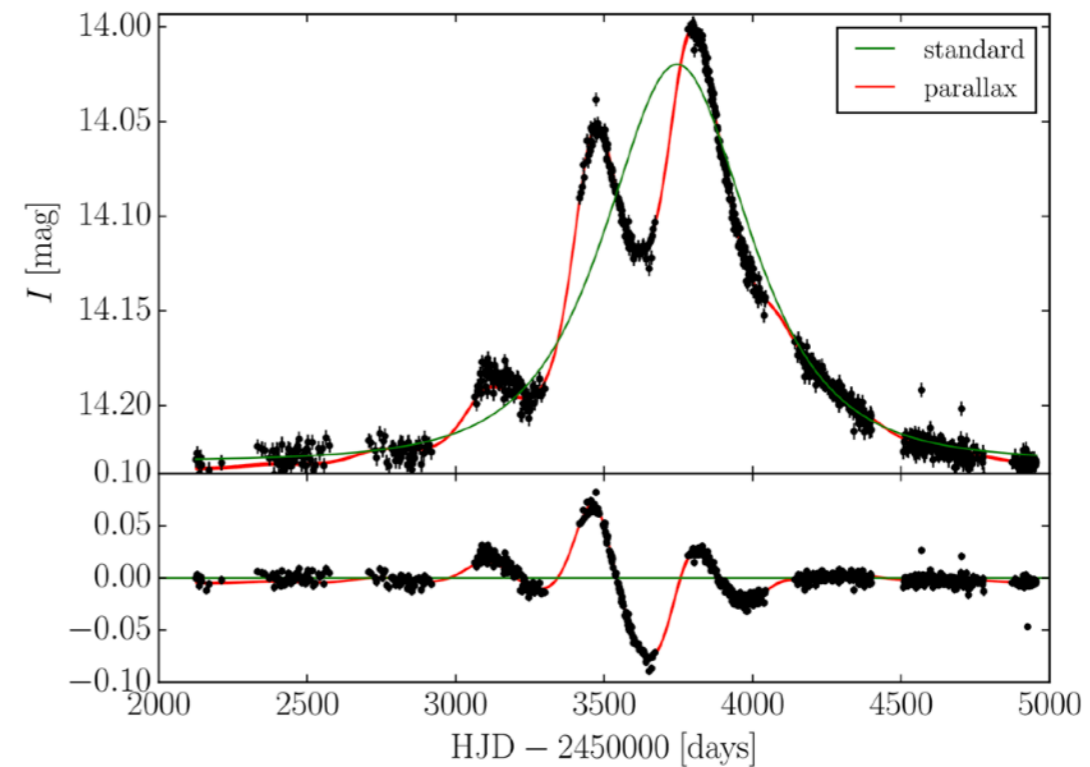
- Systematics in individual light curves
  - Microlensing + baseline variability (Gaussian processes)
- Oversimplistic modeling: point-source point-lens (PSPL)
  - Including microlensing parallax due to Earth's motion
- Using point estimates from individual events:  $t_E$  histograms
  - Forward modeling the simulated chains to infer  $t_E$  distribution
- **10,000 OGLE-III and IV events:** previous analyses overestimated the number of  $t_E > 100$  d due to ignoring parallax, black holes candidates...

# 1 Introduction

- **Timeline:** Paczynski (1986) → population of dark objects (e.g. MACHOs) → time-domain photometric surveys → dense field photometry, difference imaging photometry, alerts → LSST, Roman
- **PSPL challenges:** blended flux (1–1.5'' typical seeing), baseline variability\* (stellar, systematics), seasonal gaps, parallax\*



By B.S. Gaudi,  
Microlensing Source website



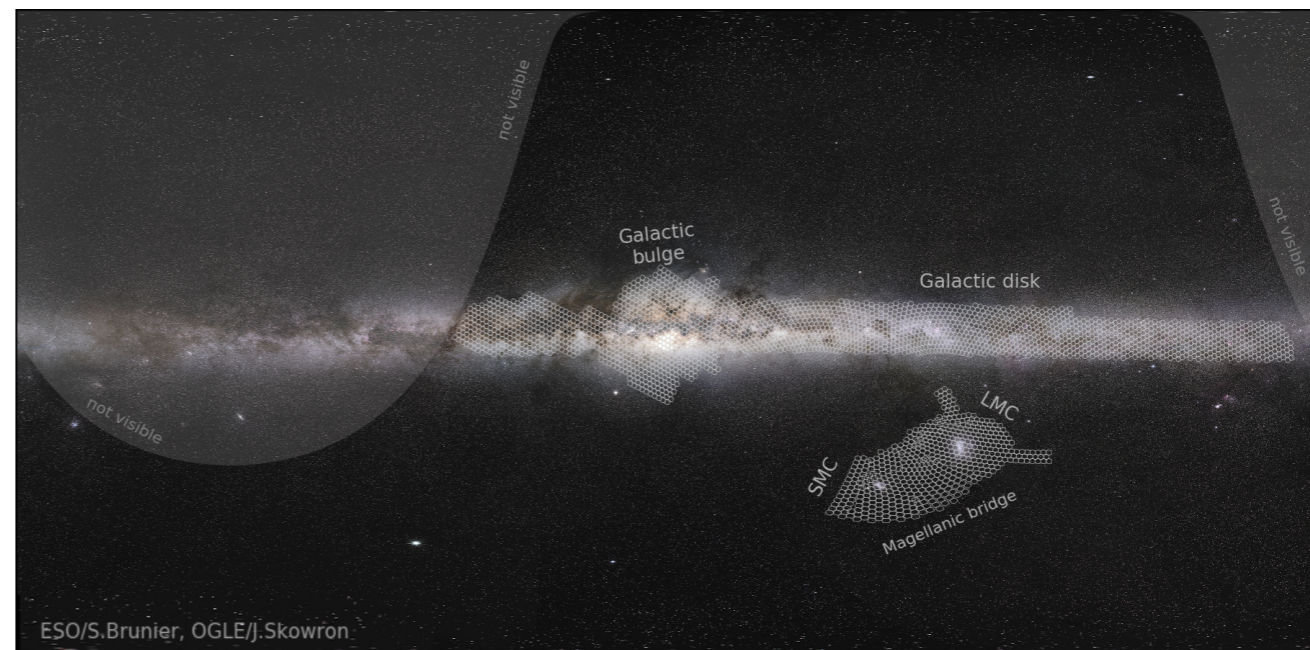
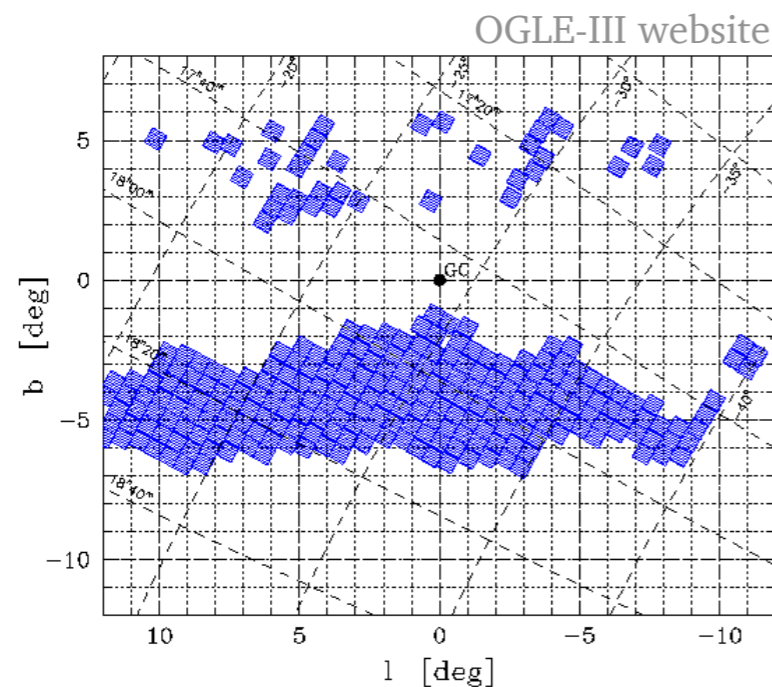
Wyrzykowski et al. (2016)

# 1 Introduction

- **Timeline:** Paczynski (1986) → population of dark objects (e.g. MACHOs) → time-domain photometric surveys → dense field photometry, difference imaging photometry, alerts → LSST, Rubin
- **PSPL challenges:** blended flux (1–1.5" typical seeing), baseline variability\* (stellar, systematics), seasonal gaps, parallax\*
- **Degeneracies:** mass-distance deg. is broken with parallax inclusion; others e.g. finite source, binary lens caustics, mass- $\mu_{\text{rel}}$ /velocity...
- **Large statistics:** distribution of Einstein crossing time ( $t_E$ ), optical depth and event rate. Distribution of  $t_E$  is dependent on the line-of-sight distribution of parallax and relative proper motion:
  - Wyrzykowski et al. (2015):  $t_E$  histogram peaks at  $\sim 27$  d
  - Mróz et al. (2019): optical depth  $\sim 10^{-6}$ , event rate =  $10^{-5}$ – $10^{-6}$  yr $^{-1}$

## 2 Data

- **OGLE-III (2002-2009):** 8 CCDs, 35' x 35' field of view. Wyrzykowski et al. (2015) detected 3560 microlensing events with PSPL fits
- **OGLE-IV (2010-):** 32 CCDs, 1.4 deg<sup>2</sup>. Mróz et al. (2019) report 5790 events



- **PopSyCLE (Lam et al. 2020):** resolved microlensing (photometric/astrometric) simulations, including evolution and compact objects →  $t_E$  distribution

### 3 Event modeling: PSPL

- Observables in the light curve:  $t_0$ ,  $u_0$  and  $t_E$  (plus  $I_0$  and  $f_s$ )
- Paczynski (1996) model for magnification:

$$A = \frac{u^2 + 2}{u\sqrt{u^2 + 4}}, \text{ where } u = \sqrt{u_0^2 + \frac{(t - t_0)^2}{t_E^2}}$$

- The mass and distance of the lens comes from the lens equation:

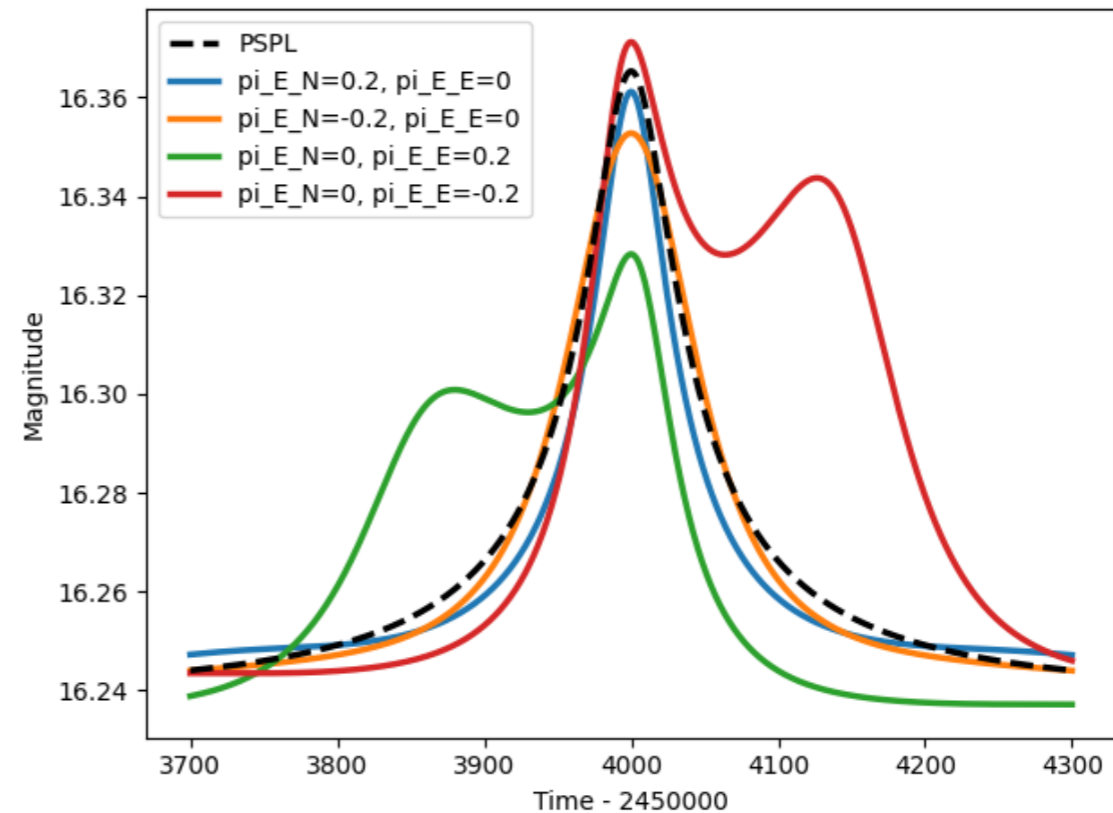
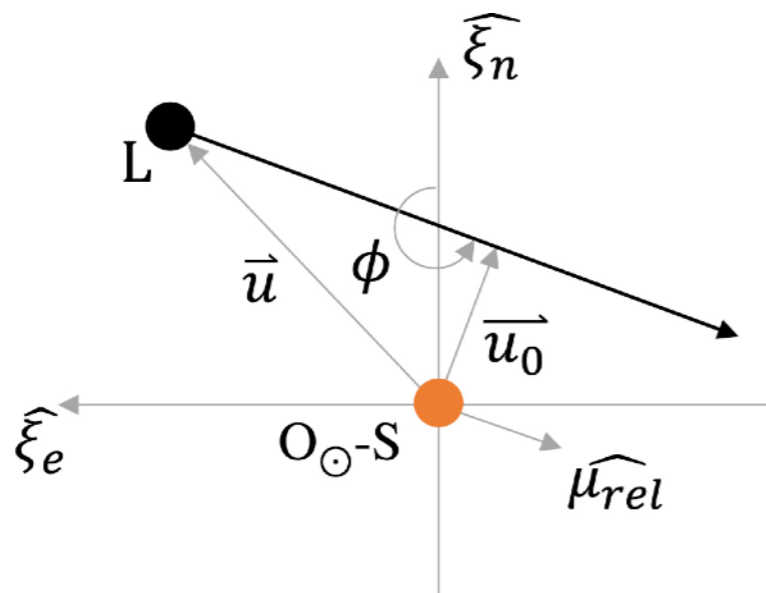
$$\theta_E = \sqrt{\frac{4GM}{c^2} \frac{D_S - D_L}{D_L D_S}}$$

- Relatively simple to model, but parallax signal starts to be detectable around  $> 30$ - $40$  days depending on the magnification ( $u_0$ ,  $t_E$ )

### 3 Event modeling: microlensing parallax

- The observer's perspective of the lens-source separation changes more quickly or slower than expected: variations in the amplifications of PSPL
- Two extra parameters: ( $\pi_{E,N}$ ,  $\pi_{E,E}$  components) or ( $\pi_E$ ,  $\phi$  angle)
- $\pi_{E,N}$  introduces symmetric distortion (harder to distinguish),  $\pi_{E,E}$  introduces asymmetries around the peak

$$M = \frac{\theta_E}{\kappa \pi_E}, \quad \kappa = 8.144 \text{ mas}/M_\odot$$



### 3 Event modeling: gaussian processes

- In this case, it is used to handle the variable baseline and correlated noise, to get more accurate model estimates without losing the parallax signal
- Probability distribution over possible functions. In practice, a stationary kernel function  $k$  is added to the covariance matrix:

$$F(t) = \text{physics}(t) + \text{GP}(t) + \text{white noise}$$

$$\Sigma_{ij} = \kappa(|t_i - t_j|) + K^2 \sigma_i^2 \delta_{ij} \quad (\text{similarity measure between two points})$$

$$p(\mathbf{F}|\boldsymbol{\theta}) = \frac{1}{(2\pi)^{N/2} |\boldsymbol{\Sigma}|^{1/2}} \exp \left[ -\frac{1}{2} (\mathbf{F} - \boldsymbol{\mu})^\top \boldsymbol{\Sigma}^{-1} (\mathbf{F} - \boldsymbol{\mu}) \right]$$

$$\boldsymbol{\Sigma} = \begin{pmatrix} k(t_1, t_1) & \dots & k(t_1, t_N) \\ k(t_2, t_1) & \dots & k(t_2, t_N) \\ \vdots & \ddots & \vdots \\ k(t_N, t_1) & \dots & k(t_N, t_N) \end{pmatrix} + \begin{pmatrix} \sigma_1^2 & 0 & \dots & 0 \\ 0 & \sigma_2^2 & \dots & 0 \\ \vdots & \vdots & \ddots & \vdots \\ 0 & 0 & \dots & \sigma_N^2 \end{pmatrix}$$

(Summary: Rasmussen & Williams 2005)  
(Other: Wyrzykowski et al. 2006, Lee et al. 2019)

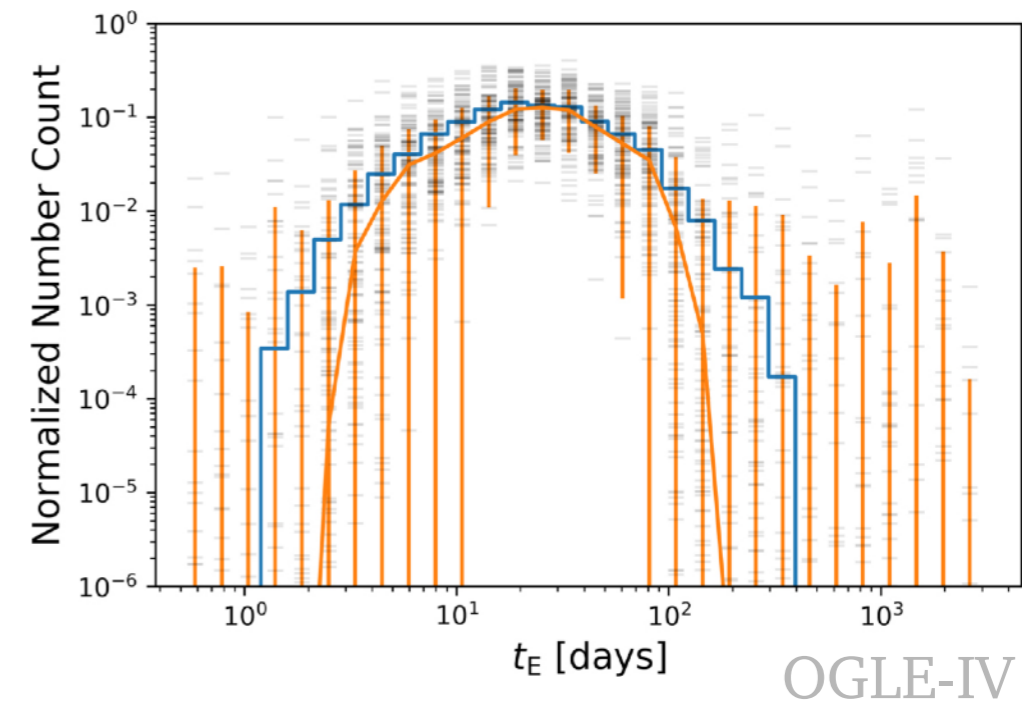
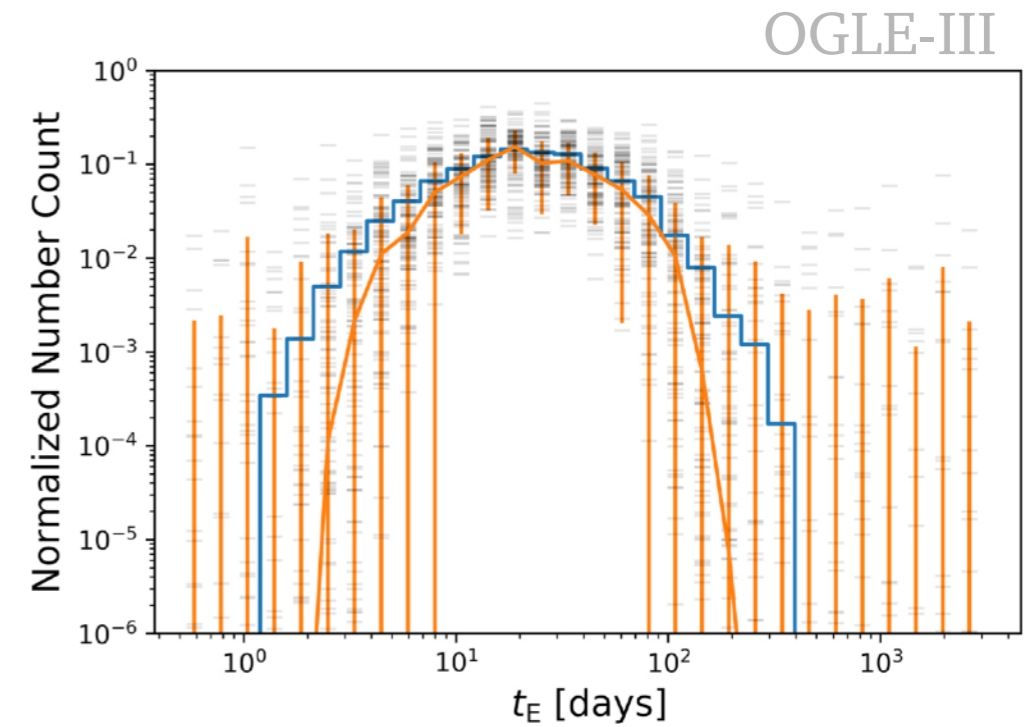
- Kernels: damped simple harmonic oscillator ( $S_0, \omega_0$ ), Matérn-3/2 ( $\sigma, \rho$ )



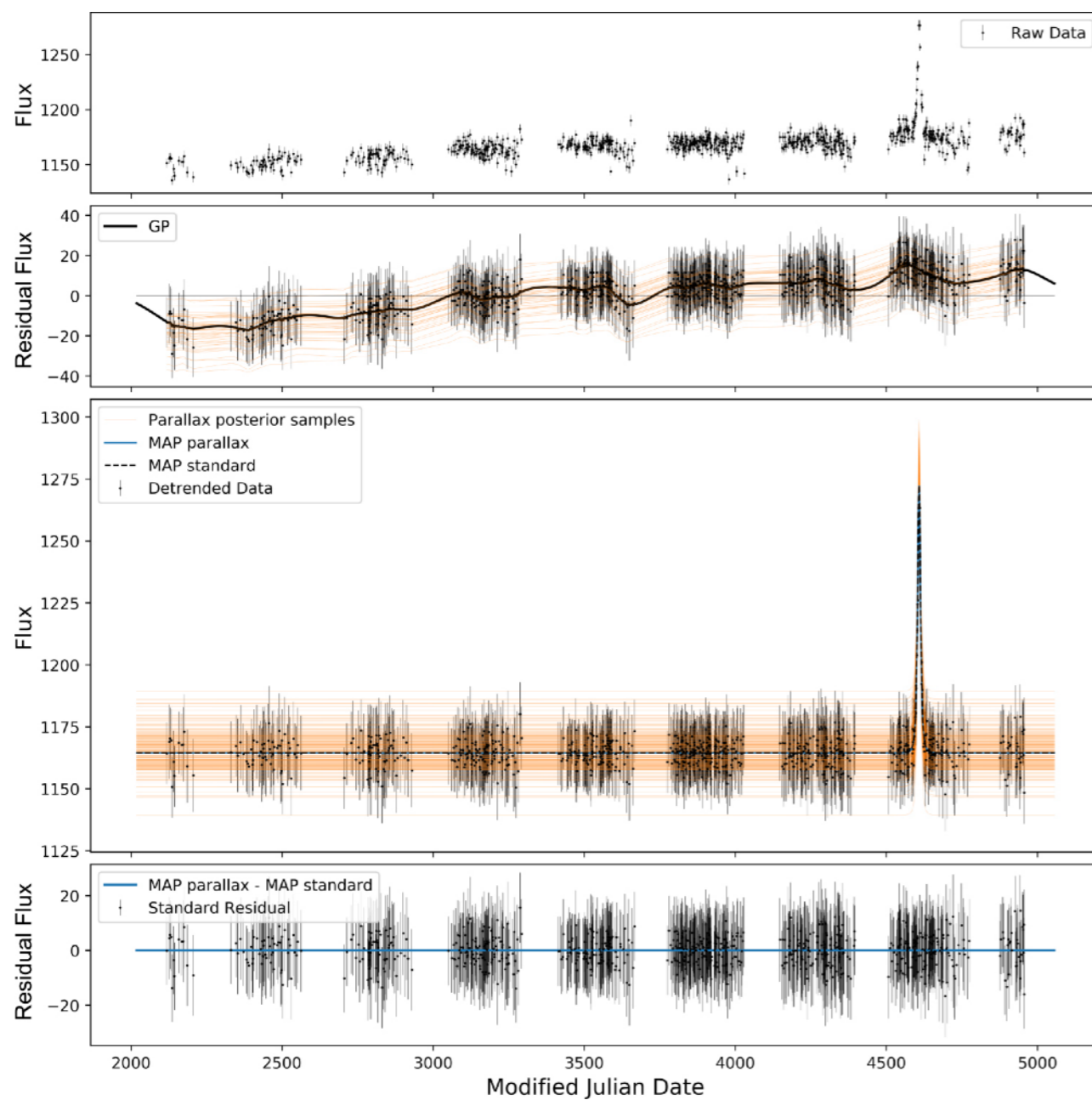
# 3 Event modeling: assumed priors

**Table 1**  
Summary of Prior Probability Density Functions for Modeled Parameters

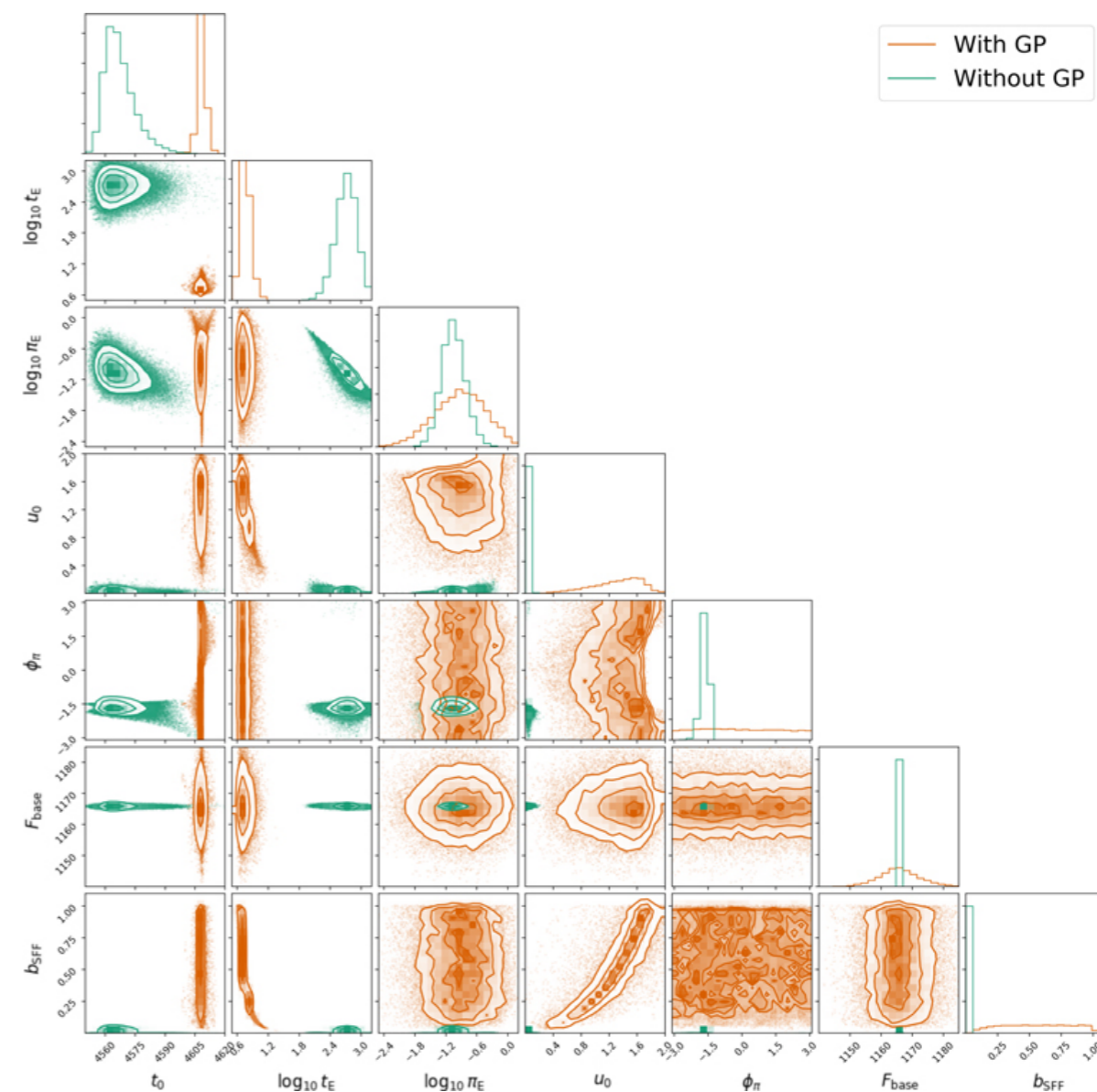
Parameter (1)	Distribution (2)	Inputs (3)
$F_{\text{base}}$	$\mathcal{N}$	$\mu = \text{med}(\mathbf{F}), \sigma = \sigma_F$
$b_{\text{sff}}$	$\mathcal{U}$	lower = 0, upper = $1 + \epsilon_{\text{NB}}$
$t_0$	$\mathcal{N}$	$\mu = t_{0,\text{OGLE}}, \sigma = 100$ days
$\log_{10} t_E$	$\mathcal{N}$	$\mu = 1.13435, \sigma = 0.67502^{\text{a}}$ , truncated between $0.5 < t_E < 3000$ days
$\log_{10} u_0$	$\mathcal{N}$	$\mu = -1, \sigma = 2$ , truncated between $10^{-5} < u_0 < 3$
$\log_{10} \pi_E$	$\mathcal{N}$	$\mu = -0.884205, \sigma = 0.072755^{\text{a}}$ , truncated between $10^{-5} < \pi_E < 3$
$\phi$	$\mathcal{U}$	lower = 0, upper = $2\pi$
$\log(S_0 \omega_0^4)$	$\mathcal{N}$	$\mu = \sigma_F^2, \sigma = 5$
$\log \omega_0$	$\mathcal{N}$	$\mu = 0, \sigma = 5$
$\log \sigma$	$\mathcal{N}$	$\mu = 0, \sigma = 5$
$\rho$	$\Gamma^{-1}$	see Section 3.3.8 for details
$\log(K^2)$	$\mathcal{N}$	$\mu = 0.0953, \sigma = 1$



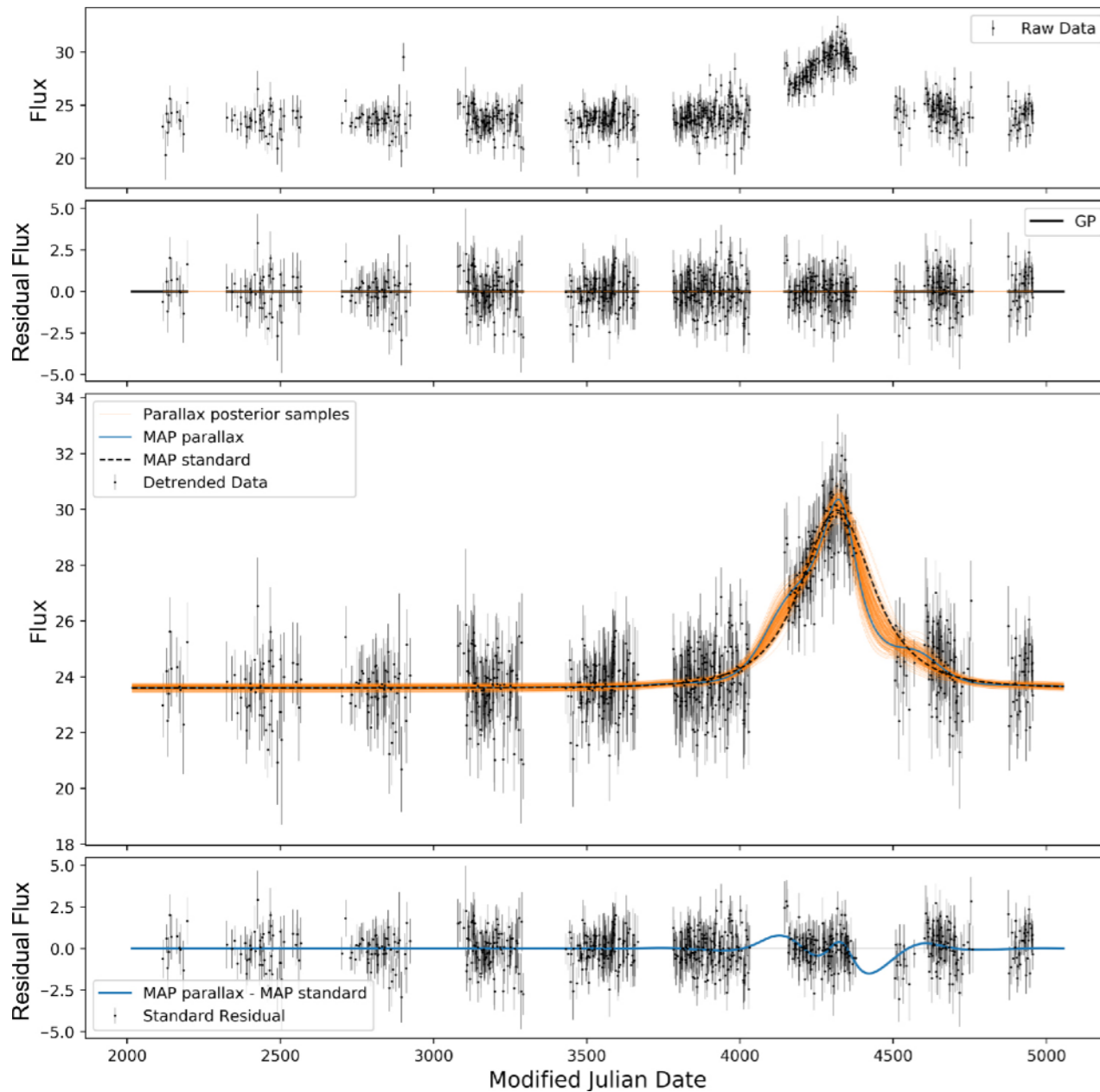
# 5 Results: OGLE BLG 156.7.141434



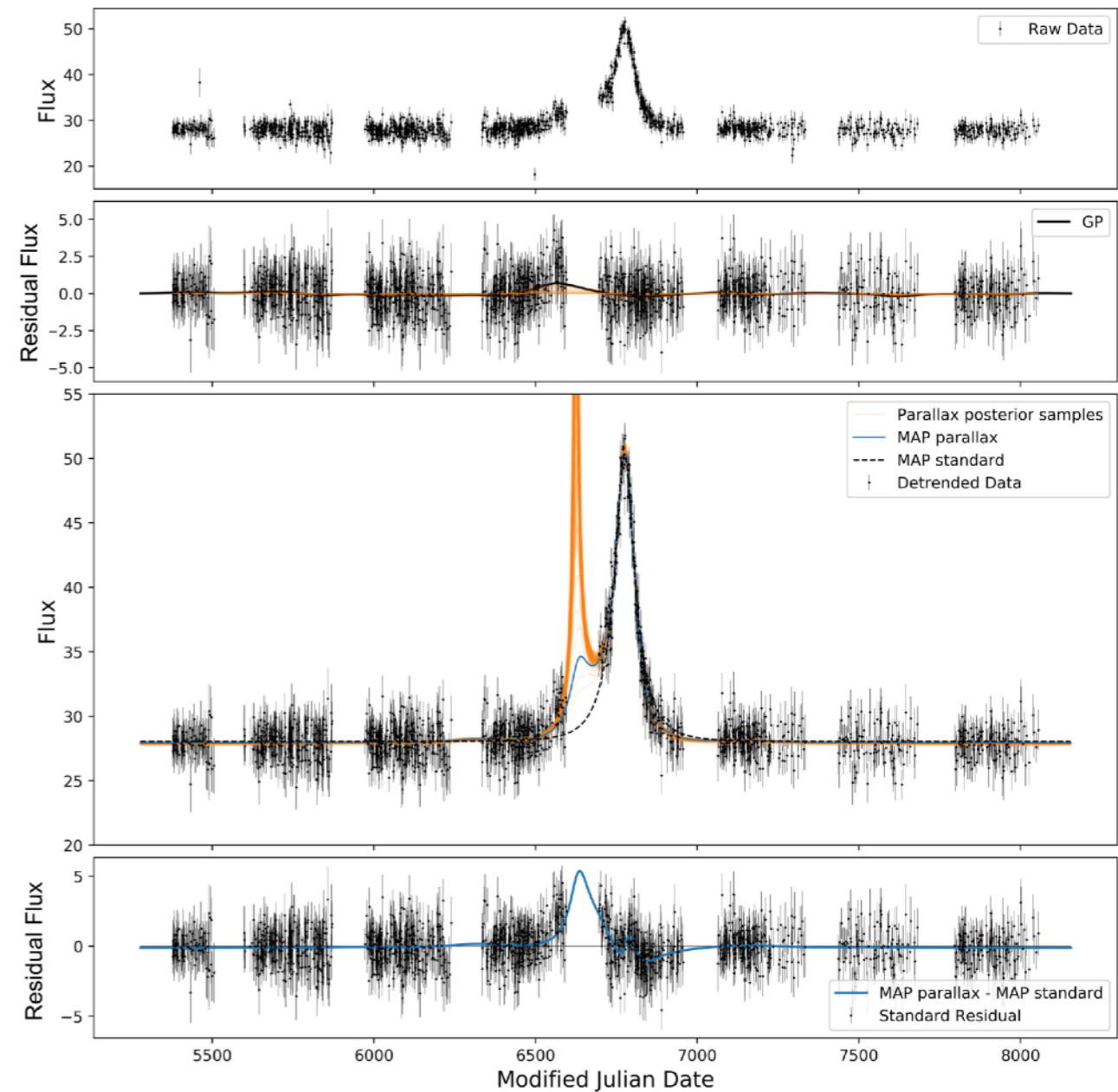
- Large baseline variation
- Small parallax signal



# 5 Results: BLG 122.6.83113 and 514.15.53029

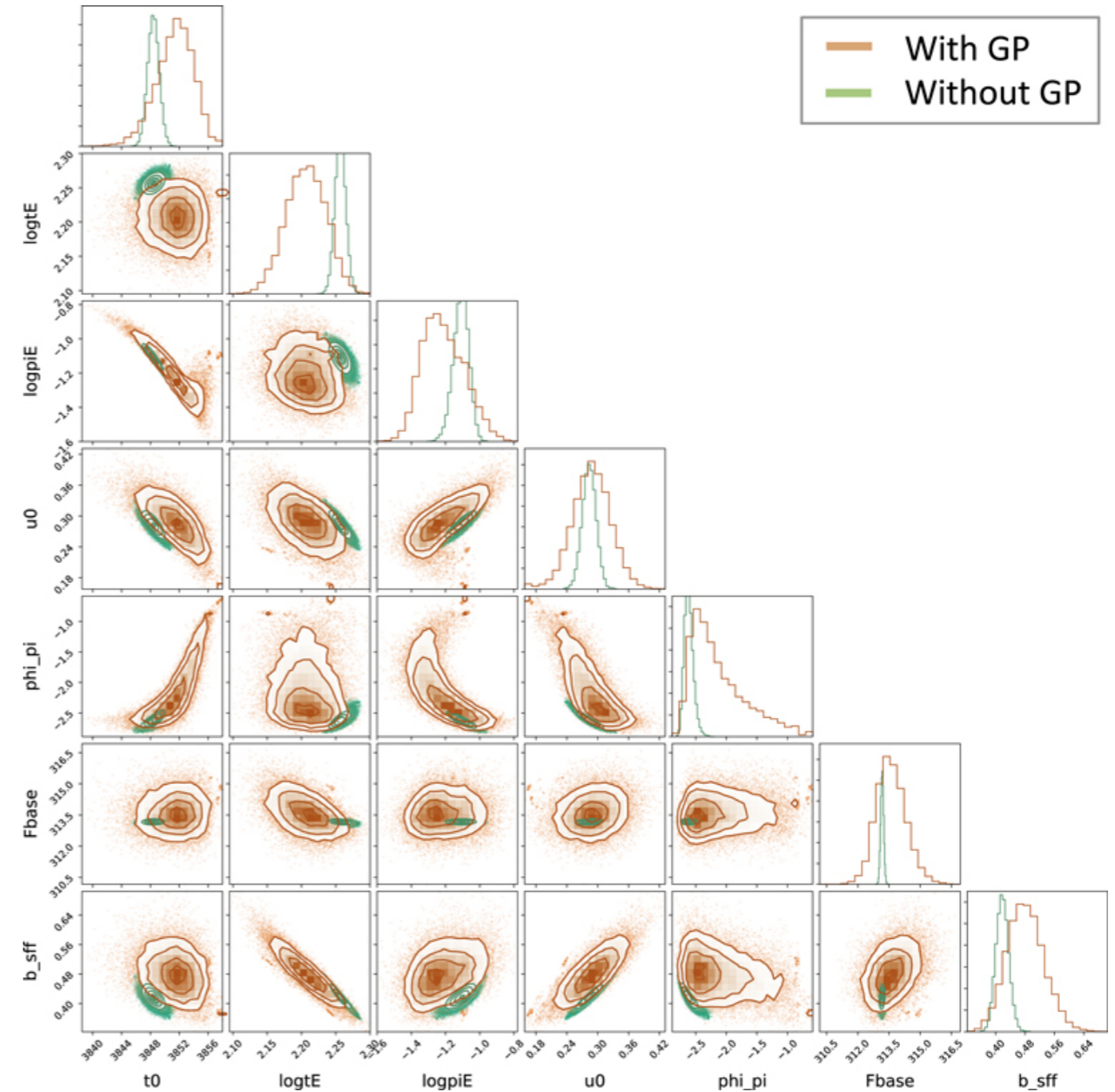
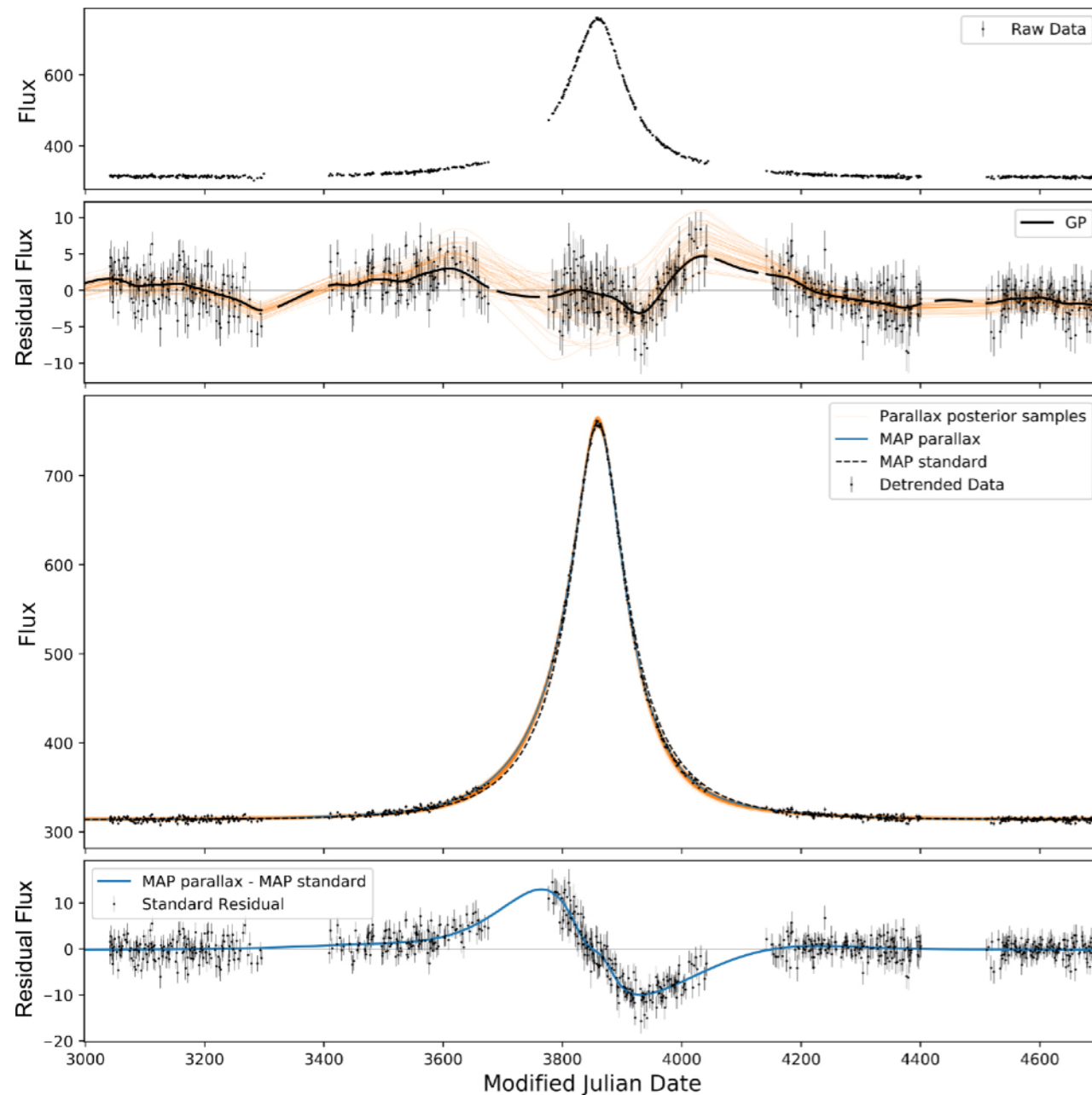


- No baseline variation
- Parallax signal in the gaps (likel. ratio=4.8)



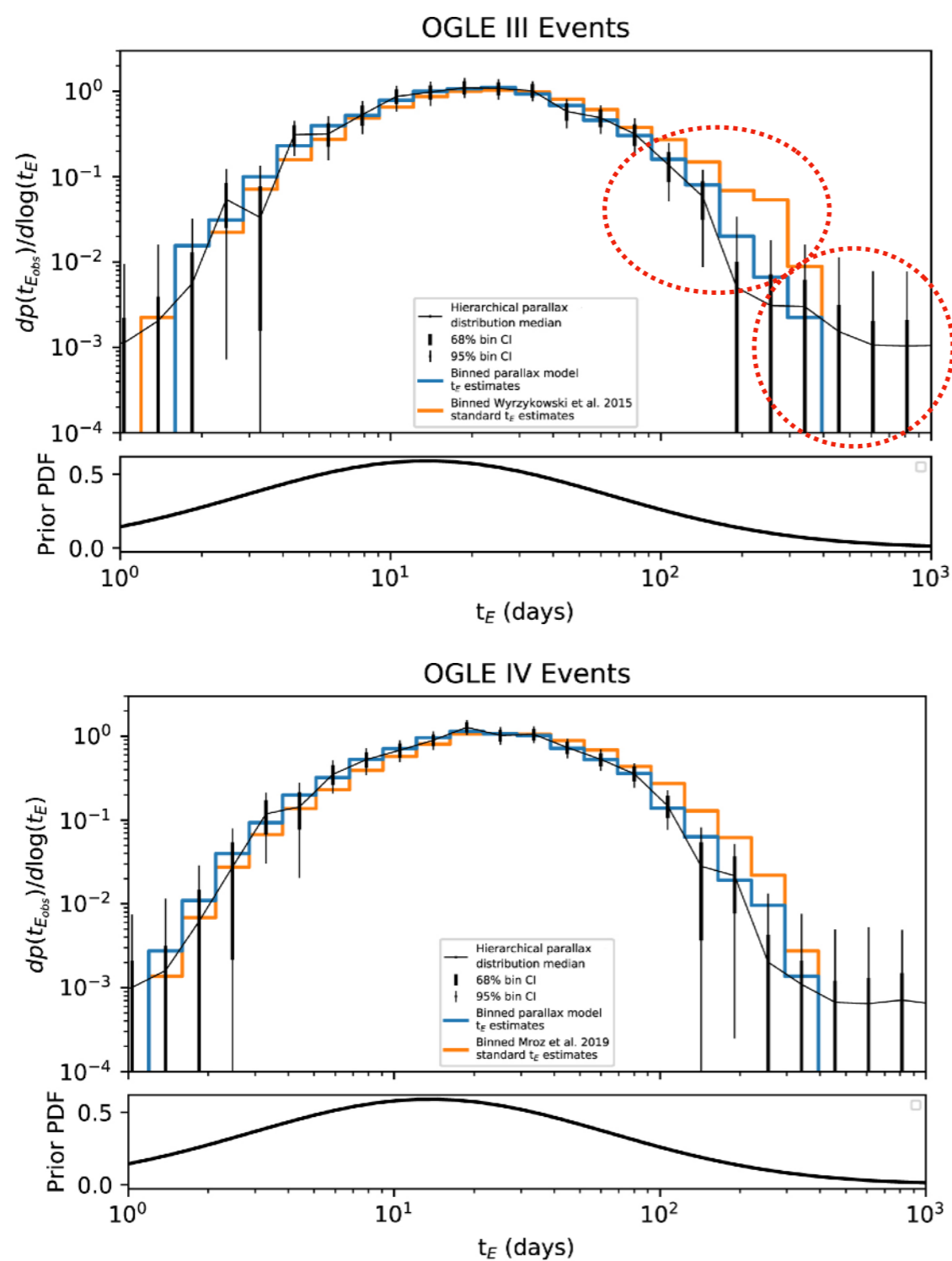
- Small baseline variation
- Samples different than best parallax

# 5 Results: OGLE BLG 102.7.44461



- Large baseline variation, strong parallax signal (likel. ratio=30), extended posteriors

# 5 Results: population modeling



- Instead of getting the maximum likelihood or the median values for the  $t_E$  distribution, the authors use all the  $t_E$  chains to forward model the distribution
- $N$  events,  $M_n$  flux measurements ( $1 \leq j \leq M_n$ ). The likelihood for a set of parameters  $\alpha$  that describe the  $t_E$  distribution:

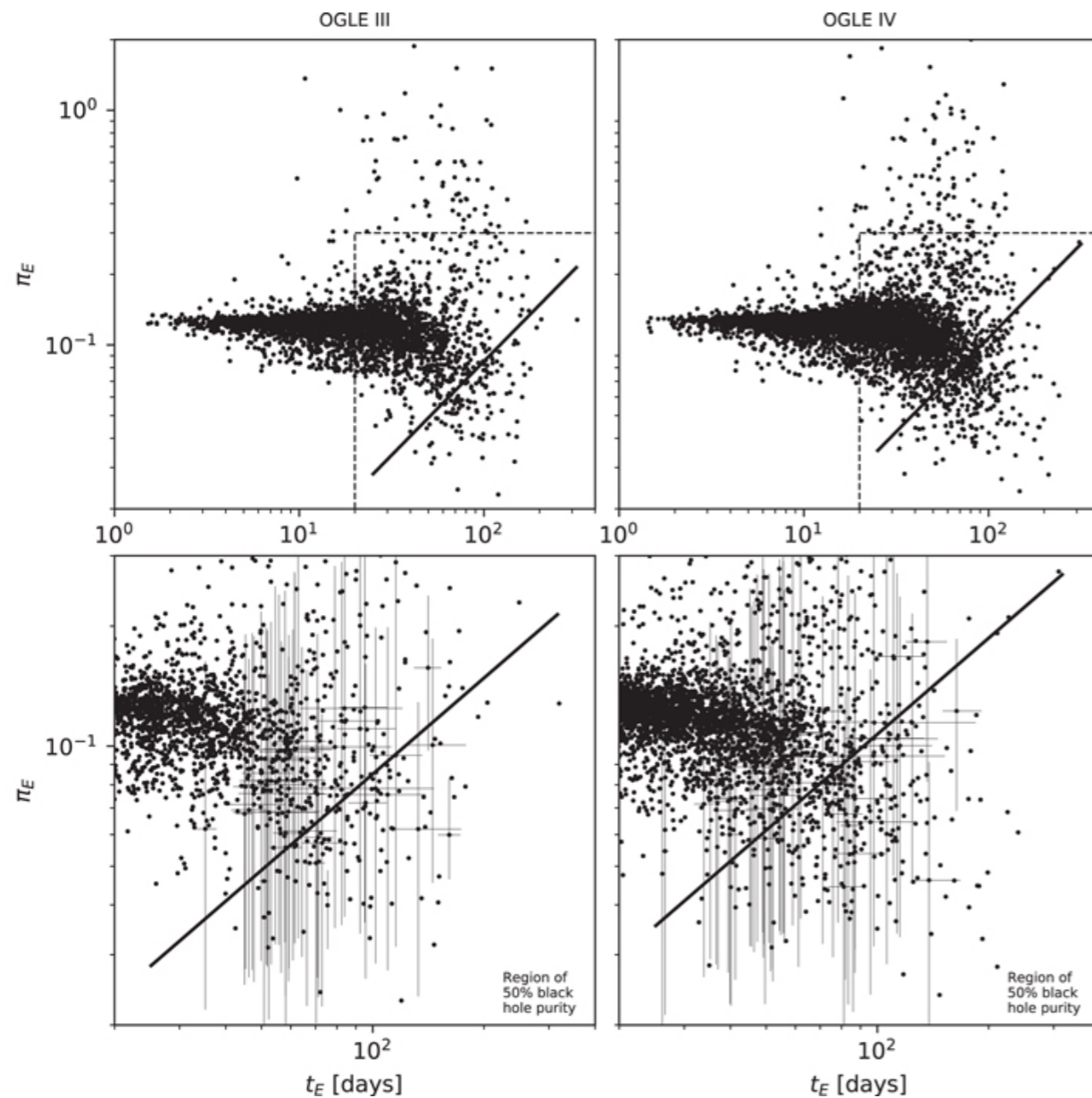
$$\mathcal{L}_\alpha \equiv p(\{F_n\}_{n=1}^N | \alpha) = \prod_{n=1}^N \int d\theta_n p(F_n | \theta_n) p(\theta_n | \alpha)$$

$$p(\theta_n | \alpha) = \frac{f_\alpha(t_E) p(\theta_n)}{p(t_E)}$$

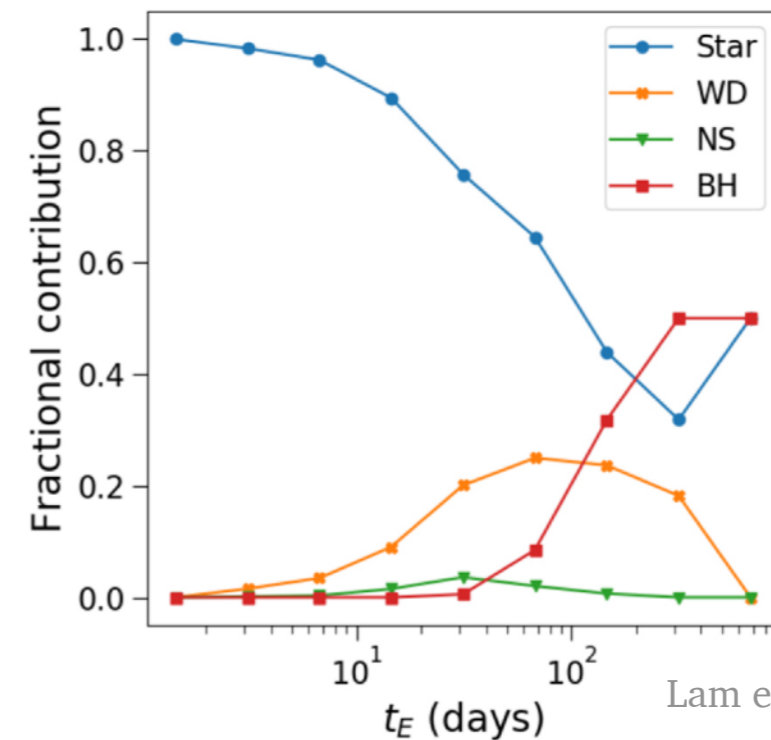
$$f_\alpha(\log_{10}(t_E)) \equiv \sum_{m=1}^M \alpha_m s\left(t_E; \frac{m-1}{M}, \frac{m}{M}\right),$$

$$s(x; L, H) \equiv \begin{cases} 0, & \text{for } x < L \\ (H - L)^{-1}, & \text{for } L \leq x \leq H, \\ 0, & \text{for } H < x \end{cases} \quad \begin{array}{l} \text{(Normalized histogram} \\ \text{with } M \text{ equal width bins} \\ \text{in } \log_{10}(t_E)) \end{array}$$

# 5 Results: black hole candidates

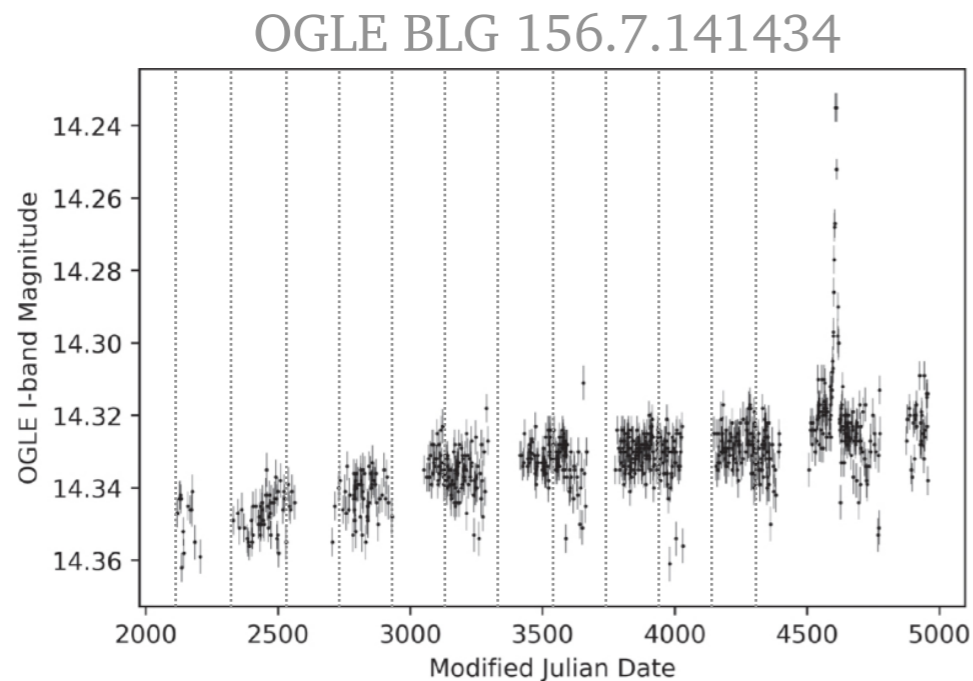


- Large error bars, but 107 candidates in OGLE-III and 283 in OGLE-IV
- Lam et al. (2020, PopSyCLE): region of largest occurrence of black holes and other stellar remnants... Above  $t_E > 100$  d, the fractional contribution of stars and black holes are almost 50-50.



Lam et al. (2020)

# - Bonus: tests to deal with the variable baseline



- *Test 1:* use increasingly smaller time intervals (also common in 2L1S methods). While the original data returns  $t_E \sim 2000$  days, the ones with smallest time intervals result in  $t_E = 70-200$  days
- *Test 2:* correct the variable baseline with a linear regression, resulted  $t_E = 6$  d

